

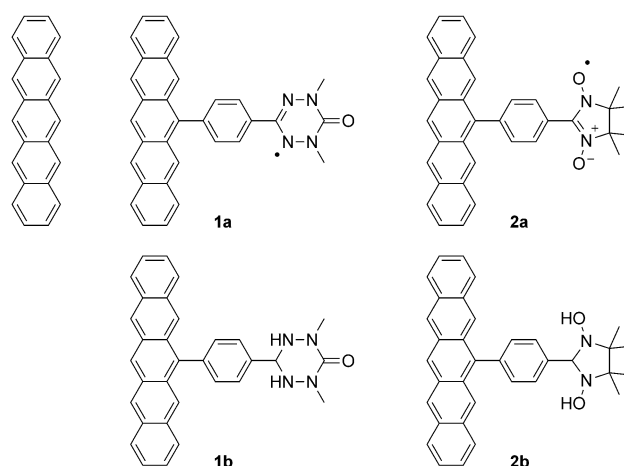
# Using Stable Radicals To Protect Pentacene Derivatives from Photodegradation\*\*

Yusuke Kawanaka, Akihiro Shimizu, Tetsuro Shinada, Rika Tanaka, and Yoshio Teki\*

Organic transistors and organic devices have a variety of applications in molecular electronics<sup>[1–3]</sup> and in the up-and-coming area of organic molecular spintronics.<sup>[4]</sup> The use of inexpensive and facile ink-jet methods<sup>[5]</sup> is possible for the fabrication of organic semiconductors. Pentacene and its derivatives<sup>[6,7]</sup> have attracted increasing interest as promising electronic materials owing to their high hole mobility.<sup>[8]</sup> Pentacene is the most promising candidate for organic field-effect transistor (OFET) applications.<sup>[3,8]</sup> However, its chemical instability in the presence of light and air<sup>[9]</sup> prevents practical applications. Efforts have been made to improve the stability by the addition of substituents.<sup>[6,7]</sup> The most notable example is 6,13-bis(triisopropylsilyl)ethynylpentacene,<sup>[7,10]</sup> in which the 6- and 13-positions of pentacene are protected by triisopropylsilyl ethynyl groups. For this pentacene derivative, extremely high hole mobility of  $1.8 \text{ cm}^2 \text{ V}^{-1} \text{ s}^{-1}$  was reported for the thin film.<sup>[8]</sup> However, the addition of substituents to photoactive carbon sites prevents further functional modifications because both the 6- and 13-positions are blocked by the substituents and also the characteristic nature of the pentacene moiety is changed.

Herein, we report a new method that utilizes a stable radical to protect pentacene derivatives from photodegradation. During the course of our systematic studies of  $\pi$ -conjugated spin systems with high-spin photo-excited states for functional materials,<sup>[11]</sup> we have discovered that a combination of two unstable species (photoreactive pentacene and a radical) leads to remarkable protection from photodegradation and an enhancement in solubility in common organic solvents. These effects are advantageous for practical applications of acene derivatives in molecular electronic devices. Radicals are well-known energy scavengers of the photo-excited state. We have utilized this characteristic of radicals to scavenge the energy of the photoexcited state of pentacene. Two novel radical pentacene hybrids, Pen-Ph-OV (**1a**) and

Pen-Ph-NN (**2a**) and their precursors (**1b** and **2b**) were synthesized (Scheme 1; Pen, Ph, OV, and NN denote pentacene, phenyl, oxo-verdazyl radical, and nitronyl nitroxide radical moieties, respectively). We demonstrate the remarkable photochemical stability induced by the attachment of



**Scheme 1.** Pentacene, **1a**, **2a**, and their precursors **1b** and **2b**, respectively.

a radical moiety to pentacene. The electrochemical properties of pentacene required for applications in molecular electronics were conserved and photochemical instability and solubility were considerably improved by this approach.

**1a** and **2a** were synthesized from **3** in five steps (Scheme 2). The ESR spectrum of solutions of **1a** and **2a** are shown in Figure 1 a and b together with simulated spectra. Their *g* values and the hyperfine splitting (see Figure 1 caption) are coincident with those of the phenylverdazyl<sup>[12]</sup> and phenyl nitronyl nitroxide radical,<sup>[13]</sup> showing the unpaired spin localized in the radical moiety, thus, indicating that the characteristic electronic properties of the pentacene moiety do not change by the attachment of a radical moiety. The X-ray crystal structure of **1a** is shown in the Supporting Information. The molecular packing was modified compared with pentacene because the phenyl group is twisted relative to the pentacene plane. This will lead to a decrease in the electron or hole mobility in the crystals. However, the molecular packing could be improved easily by replacing the phenyl linker with another linker such as an acetylene.

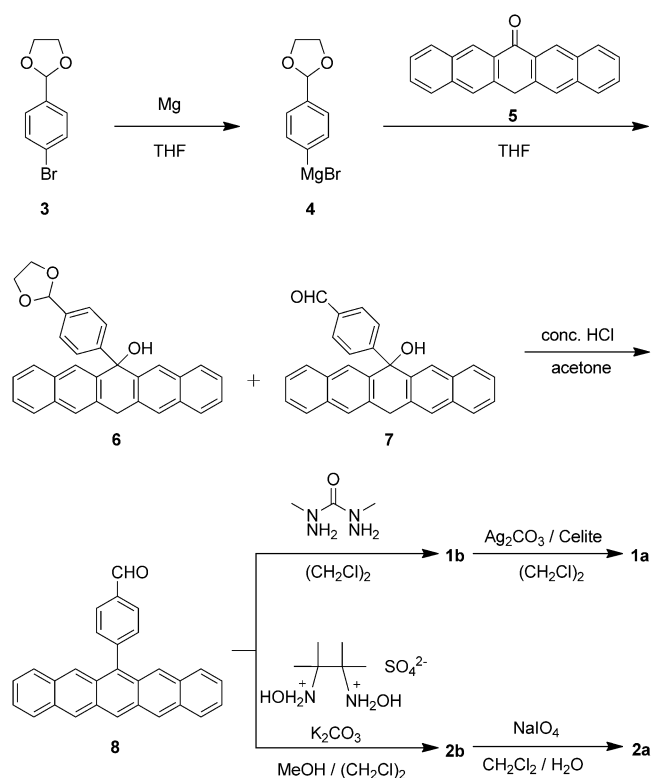
The decay profiles of the UV/Vis absorption spectra of THF solutions of **1a**, **1b**, **2a**, and **2b** under ambient light (the light of a fluorescent lamp in the laboratory) in the saturated air conditions are depicted in Figure 2. In the precursors **1b**

[\*] Y. Kawanaka, A. Shimizu, Prof. Dr. T. Shinada, Prof. Dr. Y. Teki  
Division of Molecular Material Science  
Graduate School of Science, Osaka City University  
3-3-138 Sugimoto, Sumiyoshi-ku, Osaka 558-8585 (Japan)  
E-mail: teki@sci.osaka-cu.ac.jp

Dr. R. Tanaka  
X-ray Crystal Structure Analysis Laboratory  
Graduate School of Engineering, Osaka City University  
3-3-138 Sugimoto, Sumiyoshi-ku, Osaka 558-8585 (Japan)

[\*\*] This work was supported by the Grant-in-Aid for Scientific Research (B) (No. 24350076) from Japan Society for the Promotion of Science (JSPS). We acknowledge Profs. Daisuke Kosumi and Hideki Hashimoto (Osaka City University) for their helpful discussion.

Supporting information for this article is available on the WWW under <http://dx.doi.org/10.1002/ange.201300595>.



**Scheme 2.** Synthesis routes for **1a**, **1b**, **2a**, and **2b**.

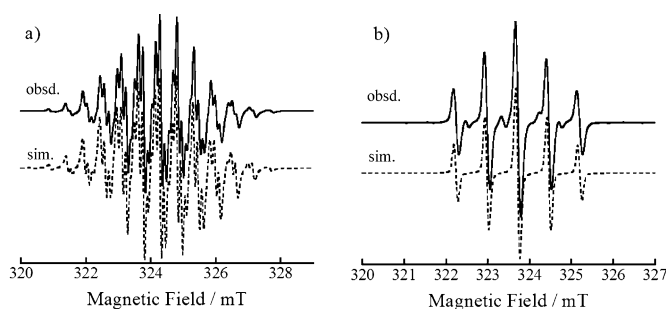


**Figure 1.** Observed and simulated X-band ESR spectra at room temperature in toluene solution. a) Spectrum of **1a**. The microwave frequency is 9.09575 GHz. The  $g$  value and hyperfine coupling constants ( $A$ ) of the nitrogen nuclei and protons of the methyl groups determined by the spectral simulation are  $g=2.0040$ ,  $A_{\text{N}}(2)=0.65$  mT,  $A_{2\text{N}}(2)=0.52$  mT, and  $A_{\text{H}}(6)=0.52$  mT, where the numbers in parentheses denote the number of equivalent nuclei. b) Spectrum of **2a**. The microwave frequency is 9.09108 GHz. The  $g$  value and hyperfine coupling constants ( $A$ ) determined by the spectral simulation are  $g=2.0065$  and  $A_{\text{N}}(2)=0.750$  mT.

and **2b**, the absorption band at 460–610 nm, which is characteristic of the pentacene moiety, decayed rapidly within a few minutes because of photochemical instability similar to that of pentacene. In contrast, almost no change was observed for **1a** under the same conditions, showing the remarkable protection from photodegradation provided by the stable radical. In addition, **1a** was easily dissolved in THF,

which is commonly used as a solvent in organic syntheses, because of the polarity of the radical moiety. Thus, issues with the solubility of pentacene for device fabrication were simultaneously solved by the attachment of the radical moiety. Similar protection from photodegradation (see Figure 2c and Figure 2d) and improvement in solubility were observed for **2a**. We also confirmed these characteristic phenomena for  $\text{CH}_2\text{Cl}_2$  solutions (see the Supporting Information, Figures S4 and S5). Figure 3 shows the decay profiles of the low-energy absorption band of  $\lambda = \text{ca. } 590$  nm of **1a**, **1b**, **2a**, and **2b** in the air-saturated THF solution (see the Supporting Information, Figure S5 for the air-saturated  $\text{CH}_2\text{Cl}_2$  solution). The accurate wavelengths of the low-energy  $\lambda_{\text{max}}$  are listed in Table 1 as well as the decay time ( $\tau$ ) obtained from the least square fitting by using the following equations;

$$A(t)/A(0) = \exp(-t/\tau) \quad \text{or} \quad (1)$$

$$A(t)/A(0) = \alpha \exp(-t/\tau_1) + (1-\alpha) \cdot \exp(-t/\tau_2), \quad (2)$$

where  $A(t)$  is the absorbance of the low-energy  $\lambda_{\text{max}}$  at time  $t$  and  $\alpha$  is the purity of the radical and the contribution of  $(1-\alpha)$  comes probably from the precursor, because the lifetime,  $\tau_2$ , is close to that of the precursor. The lifetime of **1a** is approximately 202 times (ca. 235 times for  $\tau_1$ ) longer than that of **1b** in THF and approximately 384 times (ca. 480 times for  $\tau_1$ ) longer in  $\text{CH}_2\text{Cl}_2$ , thus showing the remarkable protection provided by the radical component. No notable photostabilization was observed for 6-phenylpentacene (see the Supporting Information). These results show clearly that the present photo-stabilization does not come from the steric buffering. Similarly, the lifetime of **2a** was approximately 380 times (ca. 400 times for  $\tau_1$ ) longer than that of **2b** in THF. The photochemical stability of **2a** was 500 times better than that of pentacene in THF solution. **2a** was more stable in  $\text{CH}_2\text{Cl}_2$  (the lifetime determined from the least-square fitting of the decay is 2077 min for **2a**). The corresponding data for a  $\text{CH}_2\text{Cl}_2$  solution of pentacene could not be obtained because pentacene is not soluble in  $\text{CH}_2\text{Cl}_2$ .

To investigate the electrochemical properties, cyclic voltammetry (CV) measurements were carried out (see the Supporting Information, Figure S6). The redox potentials of **1a**, **1b**, **2a**, and **2b** are listed in Table 1, and show that the electrochemical properties of the pentacene moieties in these compounds are similar to those of pentacene. The first oxidation potential of the verdazyl radical overlaps with that of the pentacene moiety (**1a**, 294 mV).<sup>[12]</sup> In contrast, the first oxidation potential of the nitronyl nitroxide radical is split from that of the pentacene moiety<sup>[13,14]</sup> (see **2a**, 298 mV and 408 mV; see the Supporting Information, Figure S6c). A similar situation also occurs for the first reduction potentials. It is difficult to measure the redox potentials of pentacene because of its insolubility. Therefore, in Table 1, we cited the electrochemical potentials of 6,13-diphenylpentacene reported in the literature (compound **9** in Ref. [7]) instead of pentacene itself. Here, half-potentials ( $E_{1/2}$ ) were reported to be  $E_{1/2}[\text{Ox}] = +682$  mV and  $E_{1/2}[\text{red}] = -1396$  mV vs. Ag/Ag<sup>+</sup>, which correspond to  $E_{1/2}[\text{Ox}] = +170$  mV and  $E_{1/2}[\text{red}] = -1910$  mV vs. Fc/Fc<sup>+</sup>. As the redox waves at ca. +290 mV,

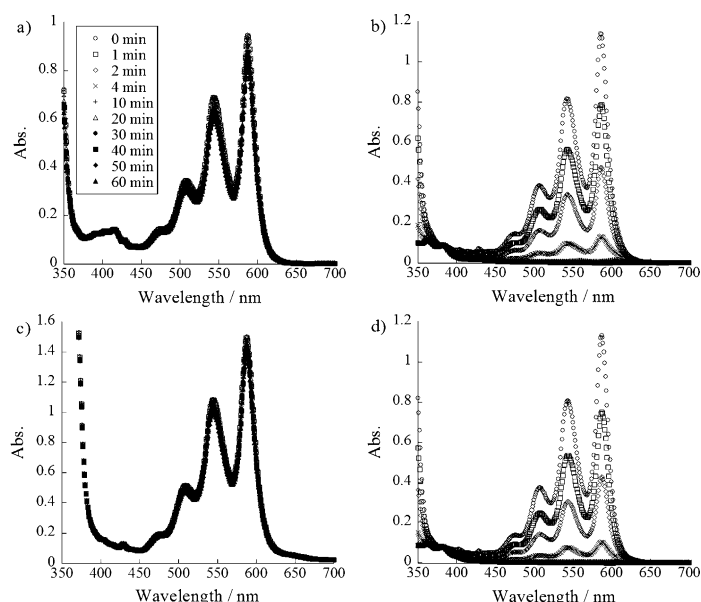


**Figure 2.** Typical UV/Vis spectra obtained at a variety of different time at room temperature under saturated air conditions in THF solutions: a) **1a** ( $0.944 \times 10^{-4}$  M); b) **1b** ( $0.945 \times 10^{-4}$  M); c) **2a** ( $1.02 \times 10^{-4}$  M); d) **2b** ( $0.983 \times 10^{-4}$  M). A typical UV/Vis spectrum for pentacene is shown in Figure S3 of the Supporting Information.

–1400 mV, and –1850 mV appeared in the cyclic voltammograms of **1a**, **1b**, **2a**, and **2b**, we assigned them to the pentacene moiety. The first oxidation and reduction potentials (the half-potentials) of the pentacene moiety of **2a**, were +298 mV (310 mV) and –1372 mV (–1450 mV) vs. Fc/Fc<sup>+</sup> (see CV curve of **2a** in the Supporting Information). The oxidation potential of **9** is expected to be lower than that of pentacene, because of the phenyl substituents, and the reduction potential to be higher. Therefore, the oxidation and reduction potentials for our compounds may be more close to those of pentacene itself. In contrast, the lifetimes of **1a** and **2a** are much longer (ca. 1090 times in CH<sub>2</sub>Cl<sub>2</sub>) than

that of pentacene. Thus, only the photochemical property was remarkably improved without loss of the electron-donor ability.

Figure 4 shows two possible mechanisms to explain this remarkable protection from photodegradation. Radical species are known as energy scavengers of the excited state because of their strong non-irradiative transition to the electronic ground state. Therefore, an effective intramolecular energy transfer from the S<sub>1</sub> state of the pentacene moiety to the D<sub>1</sub> state of the radical moiety (Pen\*(S<sub>1</sub>)–Ph–R(D<sub>0</sub>)→Pen(S<sub>0</sub>)–Ph–R\*(D<sub>1</sub>)) is expected, with subsequent rapid energy relaxation to the electronic ground state (Pen(S<sub>0</sub>)–Ph–R\*(D<sub>1</sub>)→Pen(S<sub>0</sub>)–Ph–R(D<sub>0</sub>)) by the strong non-irradiative transition, that is, the internal conversion (IC) process of the radical moiety. As shown in Figure 4, another possible mechanism is intersystem crossing (ISC) enhanced by the radical moiety; this enhanced ISC mechanism has been discussed for the  $\pi$ -conjugated spin systems in our previous work.<sup>[11a]</sup> During the energy transfer or “intersystem” crossing from Pen\*(S<sub>1</sub>)–Ph–R(D<sub>0</sub>) to the D<sub>1</sub> state of Pen\*(T<sub>1</sub>)–Ph–R(D<sub>0</sub>), the whole spin state is unchanged. Thus, spin-allowed transitions are expected, leading to the effective quench of the fluorescence of the pentacene moiety.

To clarify the mechanism, we measured fluorescence spectra (see Figure S7 in the Supporting Information). The fluorescence, resulting from the pentacene moiety, observed for **1b** and **2b** was completely quenched in the spectrum of **1a** and **2a**. The Förster mechanism<sup>[15]</sup> and other type of the energy transfer mechanisms (Dexter mechanism<sup>[16]</sup> and quantum-mechanical coherent energy-transfer mechanism<sup>[17]</sup> through  $\pi$ -conjugation) are expected to occur as well as the enhanced ISC (see the Supporting Information for further discussion). The energy transfer or enhanced ISC and subsequent strong non-adiabatic energy relaxation is a plausible mechanism for the protection of these systems from photodegradation. The lifetime of the S<sub>1</sub>-excited-state of

**Table 1:** Electrochemical (oxidation and reduction potentials,  $E[\text{Ox}]$  and  $E[\text{red}]$ ) in CH<sub>2</sub>Cl<sub>2</sub> and optical properties (low-energy  $\lambda_{\text{max}}$ , lifetime ( $\tau$ )) of pentacene and pentacene derivatives in organic solvents (THF and CH<sub>2</sub>Cl<sub>2</sub>).

	Redox potentials vs. Fc/Fc <sup>+</sup>		THF solution					CH <sub>2</sub> Cl <sub>2</sub> solution				
	$E[\text{Ox}]$ [mV]	$E[\text{red}]$ [mV]	$\lambda_{\text{max}}$ [nm]	$\tau$ [min]	$\alpha$	$\tau_1$ [min]	$\tau_2$ [min]	$\lambda_{\text{max}}$ [nm]	$\tau$ [min]	$\alpha$	$\tau_1$ [min]	$\tau_2$ [min]
Pentacene	–	–	575	$1.5 \pm 0.03$	–	–	–	–	–	insoluble	–	–
( <b>9</b> ) <sup>[c]</sup>	(+170) <sup>[b]</sup>	(–1910) <sup>[b]</sup>	–	–	–	–	–	–	–	–	–	–
<b>1a</b>	+294, <sup>[a]</sup> +908 <sup>[b]</sup>	–1380, <sup>[a]</sup> –1881	587	$404.9 \pm 12.0$	0.978	$470.4 \pm 6.4$	$4.6 \pm 0.4$	589	$768.7 \pm 32.7$	0.982	$962.9 \pm 25.3$	$4.5 \pm 0.4$
<b>1b</b>	+246, +838 <sup>[b]</sup>	–1382, –1856	586	$2.0 \pm 0.1$	–	–	–	589	$2.0 \pm 0.1$	–	–	–
<b>2a</b>	+298, +408, +861 <sup>[b]</sup>	–1372, –1580, <sup>[b]</sup> –1828	588	$728.1 \pm 12.1$	0.994	$762.6 \pm 9.2$	$2.2 \pm 0.5$	589	$1760.5 \pm 31.3$	0.993	$2076.7 \pm 51.1$	–
<b>2b</b>	+289, +850 <sup>[b]</sup>	–1349, –1863	587	$1.9 \pm 0.1$	–	–	–	589	$1.9 \pm 0.1$	–	–	–

[a] The oxidation and reduction potentials of the phenyl verdazyl radical are +270 mV and –1280 mV,<sup>[12]</sup> which are close to the potentials of **1a** (+294 mV and –1380 mV), and overlap with those of the pentacene moiety. The relative height of the oxidation wave of **1a** compared to the reduction potential is bigger than that of the precursor **1b**. [b]  $E_{1/2}$  value. [c] These data were calculated from the potentials vs. Ag/Ag<sup>+</sup> reported in Ref. [7].

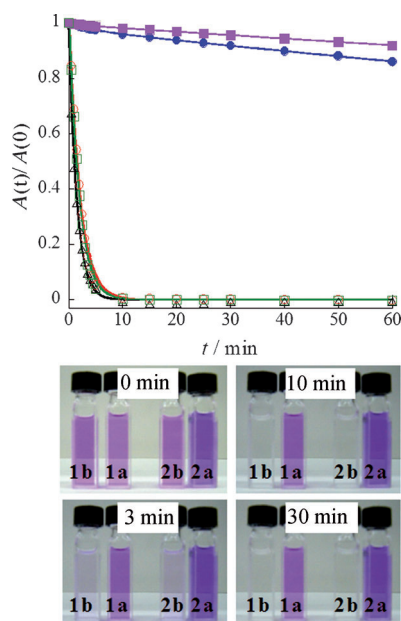


**Figure 3.** Decay profiles of the THF solutions for the characteristic absorption band of pentacene ( $\Delta$ ;  $\lambda = 575$  nm). **1a** (blue  $\bullet$ ;  $\lambda = 587$  nm), **1b** (red  $\circ$ ;  $\lambda = 586$  nm), **2a** (violet  $\blacksquare$ ;  $\lambda = 588$  nm), and **2b** (green  $\square$ ;  $\lambda = 587$  nm). Similar data for  $\text{CH}_2\text{Cl}_2$  solutions are given in the Supporting Information.

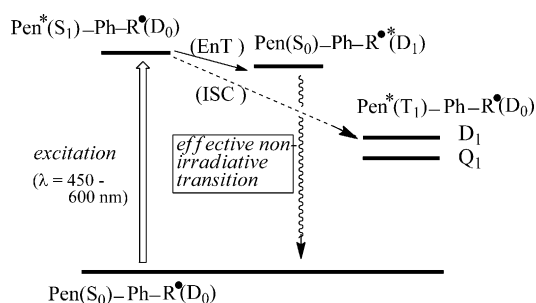


**Figure 4.** A possible mechanism for the remarkable protection from photodegradation provided by stable radicals. Efficient energy transfer occurs from  $\text{Pen}^*(\text{S}_1)\text{-Ph-R}^*(\text{D}_0)$  to  $\text{Pen}^*(\text{S}_0)\text{-Ph-R}^*(\text{D}_1)$  (from  $\text{S}_1$  excited state of pentacene moiety to  $\text{D}_1$  excited state of the radical moiety) followed by strong energy relaxation to the ground state by an effective non-irradiative transition. Enhanced ISC is also a possible mechanism.

the pentacene moiety, obtained by using an ultrafast (fs) transient absorption spectroscopy, will give more accurate information of the mechanism. The shortening of the lifetime and the contribution of the enhanced ISC mechanism have been indicated by preliminary experiments that will be published elsewhere.

As shown in Figure 2, **1a** and **2a** were easily dissolved in common organic solvents, such as THF, and  $\text{CH}_2\text{Cl}_2$ , because of the polarity of the radical moiety. This solubility is another advantage of the present protection method utilizing stable radicals. In addition, the 13-position of the pentacene moiety is free for functionalization. Radicals have an unpaired electron that can be aligned under external magnetic field.

Thus there is potential for magnetic control of hole and/or electron transport. A variety of potential applications of radical species, for example in molecular spin batteries,<sup>[18]</sup> in a high performance OFET,<sup>[19]</sup> as a photoconductive liquid-crystalline verdazyl radical,<sup>[20]</sup> and applications derived from the large negative magnetoresistance,<sup>[4]</sup> and the Kondo effect<sup>[21]</sup> were recently reported, thus opening the new research area of organic molecular spintronics. Our present method will open a promising way toward organic molecular spintronics and organic molecular electronics.

## Experimental Section

**Syntheses:** The synthesis routes to the stable radicals, **1a** and **2a**, and their precursors, **1b** and **2b** are depicted in Scheme 2. Radicals **1a** and **2a** were characterized by spectroscopic analysis. Full experimental details for the synthesis are given in the Supporting Information.

**Measurements:** UV/Vis spectra were measured on a HITACHI U-3500 at room temperature. Cyclic voltammetry (CV) was carried out in a solution of  $\text{CH}_2\text{Cl}_2$  (BuCN, 0.1M TBAPF<sub>6</sub>) by using a multipurpose electrochemical apparatus (Hokuto Denko HSV-100) under Ar in the glove box. Measurements were made using a standard three-electrode configuration comprising a glassy-carbon-disk electrode as the working electrode, a Pt wire as the counter electrode and an Ag/Ag<sup>+</sup> electrode as the reference. Ferrocene was used as internal standard. The fluorescence spectra were taken at room temperature by a HITACHI F-4500T spectrometer. A conventional X-band ESR spectrometer (JEOL TE300) was used for the cw-ESR experiment. Samples used in the ESR measurements were degassed by repeated freeze-pump-thaw cycles. X-ray diffraction data were collected on a Rigaku AFC-7/Mercury CCD area-detector diffractometer with graphite monochromated Mo-K $\alpha$  radiation ( $\lambda = 0.7107$  Å). The details are described in the Supporting Information. Ab initio molecular orbital calculations were performed using the Gaussian 09W package.<sup>[22]</sup> Ubecke 3 LYP DFT theory and 6-31G(d,p) basis sets were applied.

Received: January 23, 2013

Published online: May 21, 2013

**Keywords:** conducting materials · energy transfer · pentacene derivatives · radicals · spintronics

- [1] C. D. Dimitrakopoulos, P. R. L. Malenfant, *Adv. Mater.* **2002**, *14*, 99–117.
- [2] R. Stephen, S. R. Forrest, M. E. Thompson, *Chem. Rev.* **2007**, *107*, 923–925.
- [3] M. Mas-Torrent, C. Rovira, *Chem. Soc. Rev.* **2008**, *37*, 827–838.
- [4] M. M. Matsushita, H. Kawakami, T. Sugawara, M. Ogata, *Phys. Rev. B* **2008**, *77*, 195208.
- [5] Z. Nie, E. Kumacheva, *Nat. Mater.* **2008**, *7*, 277–290.
- [6] J. E. Anthony, *Angew. Chem.* **2008**, *120*, 460–492; *Angew. Chem. Int. Ed.* **2008**, *47*, 452–483.
- [7] I. Kaur, W. Jia, R. P. Kopreski, S. Selvarasah, M. R. Dokmeci, C. Pramanik, N. McGruer, G. P. Miller, *J. Am. Chem. Soc.* **2008**, *130*, 16274–16286.
- [8] S. K. Park, T. N. Jackson, J. E. Anthony, D. A. Mourey, *Appl. Phys. Lett.* **2007**, *91*, 063514.
- [9] J. B. Birks, J. H. Appleyard, R. Pope, *Photochem. Photobiol.* **1963**, *2*, 493–495.
- [10] J. E. Anthony, J. S. Brooks, D. L. Eaton, S. R. Parkin, *J. Am. Chem. Soc.* **2001**, *123*, 9482–9483.
- [11] a) Y. Teki, S. Miyamoto, M. Nakatsuji, Y. Miura, *J. Am. Chem. Soc.* **2001**, *123*, 294–305; b) Y. Teki, H. Tamekuni, J. Takeuchi, Y.

- Miura, *Angew. Chem.* **2006**, *118*, 4782–4786; *Angew. Chem. Int. Ed.* **2006**, *45*, 4666–4670; c) Y. Takemoto, Y. Teki, *ChemPhys-Chem* **2011**, *12*, 104–108; d) K. Katayama, M. Hirotsu, I. Kinoshita, Y. Teki, *Dalton Trans.* **2012**, *41*, 13465–13473, and references therein.
- [12] J. B. Gilroy, S. D. J. McKinnon, B. D. Koivisto, R. G. Hicks, *Org. Lett.* **2007**, *9*, 4837–4840.
- [13] E. F. Ullman, J. H. Osiecki, D. G. B. Boocock, R. Darcy, *J. Am. Chem. Soc.* **1972**, *94*, 7049–7059.
- [14] a) K. Oyaizu, T. Sukegawa, H. Nishide, *Chem. Lett.* **2011**, *40*, 184–185; b) J. Lee, E. Lee, S. Kim, G. S. Bang, D. A. Shultz, R. D. Schmidt, D. E. Forbes, H. Lee, *Angew. Chem.* **2011**, *123*, 4506–4510; *Angew. Chem. Int. Ed.* **2011**, *50*, 4414–4418.
- [15] “Zwischenmolekulare Energiewanderung und Fluoreszenz”: T. Förster, *Ann. Phys.* **1948**, *437*, 55–75.
- [16] D. L. Dexter, *J. Chem. Phys.* **1953**, *21*, 836–850.
- [17] L. Yang, S. Caprasecca, B. Mennucci, S. Jang, *J. Am. Chem. Soc.* **2010**, *132*, 16911–16921.
- [18] T. Suga, H. Ohshiro, S. Sugita, K. Oyaizu, H. Nishide, *Adv. Mater.* **2009**, *21*, 1627–1630.
- [19] Y. Wang, H. Wang, Y. Liu, C. Di, Y. Sun, W. Wu, G. Yu, D. Zhang, D. Zhu, *J. Am. Chem. Soc.* **2006**, *128*, 13058–13059.
- [20] A. Jankowiak, D. Pociecha, J. Szczytko, H. Monobe, P. Kaszynski, *J. Am. Chem. Soc.* **2012**, *134*, 2465–2468.
- [21] T. Komeda, H. Isshiki, J. Liu, Y.-F. Zhang, N. Lorente, K. Katoh, B. K. Breedlove, M. Yamashita, *Nat. Commun.* **2011**, *2*, 217.
- [22] M. Frisch, et al., Gaussian09, Rev.A.02, Gaussian, Inc., Wallingford CT, **2009**.